# Disorder line and incommensurate floating phases in the quantum Ising model on an anisotropic triangular lattice

V. I. Iglovikov, R. T. Scalettar, R. R. P. Singh, and J. Oitmaa

Phys. Rev. B **87**, 214415 — Published 13 June 2013

DOI: 10.1103/PhysRevB.87.214415

# Disorder Line and Incommensurate Floating Phases in the Quantum Ising Model on an Anisotropic Triangular Lattice

V.I. Iglovikov, R.T. Scalettar, and R.R.P. Singh
*Physics Department, University of California, Davis, California 95616, USA*

J. Oitmaa
*School of Physics, The University of New South Wales, Sydney 2052, Australia*

We present a Quantum Monte Carlo study of the Ising model in a transverse field on a square lattice with nearest-neighbor antiferromagnetic exchange interaction J and one diagonal second-neighbor interaction $J'$, interpolating between square-lattice ($J' = 0$) and triangular-lattice ($J' = J$) limits. At a transverse-field of $B_x = J$, the disorder-line first introduced by Stephenson, where the correlations go from Neel to incommensurate, meets the zero temperature axis at $J' \approx 0.7J$. Strong evidence is provided that the incommensurate phase at larger $J'$, at finite temperatures, is a floating phase with power-law decaying correlations. We sketch a general phase-diagram for such a system and discuss how our work connects with the previous Quantum Monte Carlo work by Isakov and Moessner for the isotropic triangular lattice ($J' = J$). For the isotropic triangular-lattice, we also obtain the entropy function and constant entropy contours using a mix of Quantum Monte Carlo, high-temperature series expansions and high-field expansion methods and show that phase transitions in the model in presence of a transverse field occur at very low entropy.

PACS numbers: 05.10.-a, 05.30.Rt, 75.10.Jm, 75.40.Mg,

## I. INTRODUCTION

The Ising model in a transverse magnetic field,

$$\hat{H} = +\sum_{i,j} J_{ij}\hat{S}_i^z\hat{S}_j^z - B_x\sum_i \hat{S}_i^x, \qquad (1)$$

illustrates a variety of interesting statistical mechanics behaviors in part because of the simplicity of its mapping to an equivalent classical problem in one higher dimension[1–6]. In the case when the exchange coupling $J_{ij} < 0$ is ferromagnetic, the model exhibits a quantum phase transition: increasing $B_x$ causes the emergence of a paramagnetic phase at $T = 0$. On the other hand, on a triangular lattice when $J_{ij} > 0$ is antiferromagnetic, $B_x$ can have the opposite effect and cause order to occur by removing[7] the large ground state degeneracy ($s(T = 0) \approx 0.32$) present in the zero field case[8]. The antiferromagnetic transverse field model on the isotropic triangular lattice was studied by Isakov and Moessner[9] using Quantum Monte Carlo simulations, who concluded that there are three different phases: a paramagnet and two distinct ordered phases distinguished by the relative dominance of quantum or thermal fluctuations.

Experimental motivation for the study of the transverse field Ising model dates back to deGennes[10], who considered the ferroelectric $KH_2PO_4$ in which a double well structure of the proton position corresponds to the Ising variable, and the transverse field represents inter-well tunneling[11]. Much more recently, transverse field Ising models have also begun to be realized experimentally in cold atom systems and this provides the immediate motivation for our work. The Maryland group[12] has assembled small, highly-connected clusters of trapped $^{171}Yb^+$ ions, and demonstrated a sharp crossover from paramagnetic to ferromagnetic behavior as the Ising coupling is scaled up relative to the transverse field. Similarly, the Bollinger group at NIST[13] is exploring larger collections of up to hundreds of Be ions in a Penning trap in triangular geometries with a spin-dependent optical dipole force with an adjustable power law decay. Transverse field Ising models with dipolar interactions have also been considered[14] in the context of solid state systems such as the glassy low temperature properties of $LiHo_xY_{1-x}F_4$.[15]

In this paper we calculate the thermodynamics and phase transitions in several specific instances of the transverse field Ising model in two spatial dimensions, using a combination of high temperature and high field series expansions[16,17] and continuous time Quantum Monte Carlo (CTQMC) approaches[5,9,18]. Our motivations are twofold. First, in light of the developments in cold-atom systems, we study the entropy function of the triangular lattice model with ferromagnetic and then antiferromagnetic couplings. In both cases CTQMC results are compared with high temperature and high field expansions. When $J > 0$, a key conclusion is that the ordered phases which are induced by $B_x \neq 0$ occur at very low entropy per particle $s$. For these transitions to be accessible experimentally, $s \lesssim 0.1\, k_B$ will typically be required. Longer range couplings, present in the experimental systems described above, are shown not to dramatically alter the isentropes. In particular, ordered phases, if present, will still occur only at rather low entropy.

Our second motivation is to understand how the Ising-like Neel transition in an unfrustrated system gives way to incommensurate order and Kosterlitz-Thouless type behavior as frustrating further neighbor interactions are added. For this, we consider a square

lattice model with nearest neighbor interaction $J$ and an antiferromagnetic next-nearest-neighbor interaction $J'$ along one diagonal, which then interpolates between the square and triangular lattice limits. There have been many previous studies of Heisenberg and Hubbard models in this geometry[19], but we are not aware of any previous work on the quantum Ising model except in the weakly frustrated case[20]. Indeed, this model raises several challenging questions for any numerical study, but also, as we shall demonstrate, some interesting and novel physics.

For the classical Ising model ($B_x = 0$) it is known[21,22] that there is a conventional second order phase transition for $J'<J$, but that $T_c$ vanishes for $J' \geq J$. As $J' \to J$, the critical temperature vanishes as $T_c \sim 2(J - J')/\ln 2$. The order in the low temperature phase remains commensurate in the two-sublattice pattern for all $J'/J < 1$. Stephenson introduced a disorder line in the $T/J$, $J'/J$ parameter space, where the short-range order in the system moves away from $(\pi, \pi)$. Above $J'/J = 0.6$, the disorder line comes very close to the phase transition line, but the phase transition remains pinned to the $(\pi, \pi)$ state. We would like to understand the fate of the disorder line in presence of the transverse-field $B_x$ and see if there is a resulting incommensurate order of the Kosterlitz-Thouless (KT) type as would be expected for a system with an emergent phase variable with XY symmetry as discussed by Bak and Villain[23].

In the triangular-lattice limit studied by Isakov and Moessner, the order is locked to a commensurate 3-sublattice pattern. This gives rise to 6th order anisotropies for the emergent phase variable. Although such an anisotropy is irrelevant at the finite temperature phase transition from the paramagnetic phase, thus giving rise to a KT transition with a power-law phase, it ultimately succeeds in driving the system to long-range order, hence their conclusion of 3 different phases in the model. In the $T = 0$ limit, our model is equivalent to a 3-dimensional system and therefore can have a Lifshitz point and a true incommensurate long-range ordered phase.[23] However, there can not be such a long-range ordered phase at finite temperatures. We have not studied the very low temperature limit of our model, where the system may, for some ranges of $J'/J$, lock in to different commensurate phases, thus giving rise to long-range order which could extend to some finite but very low temperatures. Our system has some similarities with the well studied ANNNI models[24] as far as the onset of incommensurate order is concerned. However, one key difference from the ANNNI models is that in the latter one particular direction is singled out by the interactions and becomes the direction in which incommensurate order and various commensurate lock-ins occur. In contrast, in our model incommensurate wave vectors and commensurate phases can have a much more two-dimensional character.

The remainder of this paper is organized as follows. In Sec. II we summarize our three calculational approaches, Quantum Monte Carlo and high temperature and high field expansions. In Sec. III we discuss the square to triangular interpolation and the nature of the phases and phase transitions. Although this is the second of the motivations presented above, we discuss it first, since it illustrates some of the rich physics introduced by frustrating interactions. We defer to Sec. IV the thermodynamics of the triangular lattice antiferromagnetic Ising model of relevance to optical lattice experiments. Sec. V summarizes our results.

## II. CALCULATIONAL APPROACHES

### A. Quantum Monte Carlo Method

We employ the CTQMC (Continuous Time Quantum Monte Carlo) algorithm described in [9]. In this method, we use the Suzuki-Trotter formalism to map a $2D$ quantum Hamiltonian, which is on a triangular lattice, onto the $3D$ classical Ising model on a stacked triangular lattice. The number of layers $L_\tau$ in the extra dimension is $L_\tau = \beta/\epsilon$, where $\beta$ represents the inverse temperature and $\epsilon$ the discretization step. The mapping becomes exact as $\epsilon \to 0$. In this limit, the number of layers becomes infinite and computationally much less intractable. However, an alternate view as $\epsilon \to 0$ is to think of consecutive spins, which have the same value along the extra dimension, as parts of continuous segments rather than living on individual, discrete lattice points. We treat these segments as our dynamical objects in the simulation. This approach makes the simulation algorithm non-local, memory efficient and allows one to work explicitly in the $\epsilon \to 0$ limit.[9,26]

Measured quantities include the real space spin correlations $C(\mathbf{r})$,

$$C(\mathbf{r}) = \langle \hat{S}^z_i \hat{S}^z_{i+\mathbf{r}} \rangle \ , \tag{2}$$

and their momentum space counterparts, the magnetic structure factor $S(\mathbf{q})$,

$$S(\mathbf{q}) = \frac{1}{N} \sum_{\mathbf{r}} e^{i\mathbf{q}\cdot\mathbf{r}} C(\mathbf{r}) \ . \tag{3}$$

We also extract the Binder ratio,

$$U_L = 1 - \frac{\langle M^4 \rangle}{3\langle M^2 \rangle^2} \tag{4}$$

where $M^2$ is the value of the structure factor at the ordering wave vector.

Entropy $s$ is measured by numerical integration of the internal energy $\langle E \rangle$

$$s(T) = \ln 2 + \frac{\langle\, E(T)\,\rangle}{T} - \int_T^\infty dT' \, \frac{\langle E(T') \rangle}{T'^2} \tag{5}$$

We have checked that our algorithm leads to data in complete agreement with exact diagonalisation results

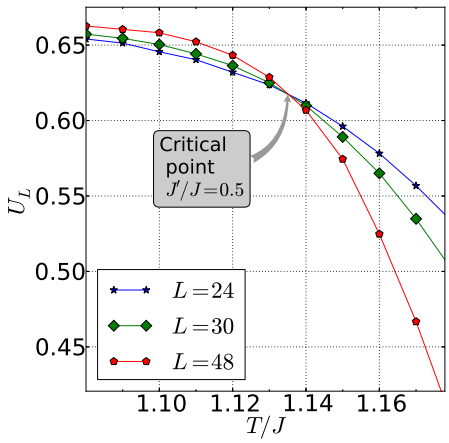


FIG. 1: (Color online) Binder crossing for $J'/J = 0.5$ at $B_x/J = 1$. For $J'/J$=0 we have the square lattice $T_c/J = 2.269$. Here the critical temperature has been suppressed by a factor of two by the frustration introduced by the next-near neighbor interaction $J'$ and by the quantum fluctuations due to $B_x$.

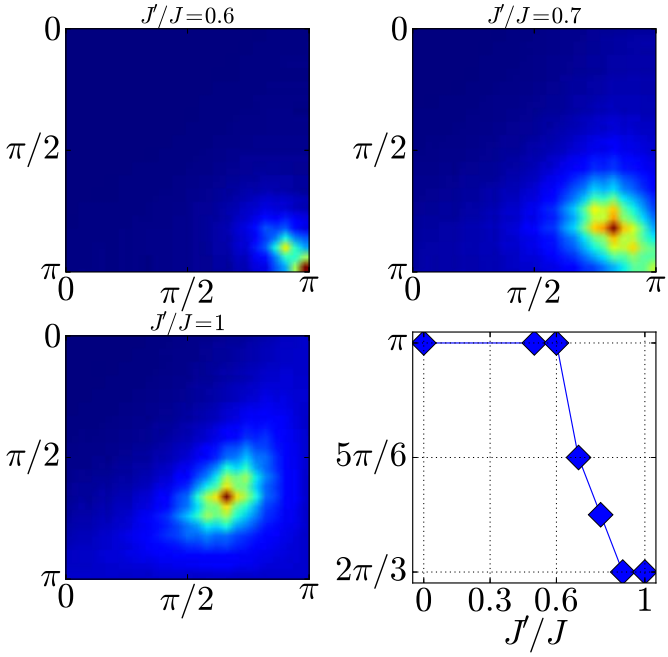


FIG. 2: (Color online) Evolution of the static structure factor with increasing $J'/J$ (ie as the triangular lattice is approached) for $B_x = 1, T = 1$. For $J'/J < 0.7$ the structure factor is peaked at the AF wavevector $\mathbf{q} = (\pi, \pi)$. The beginning of a shift away from this value is evident at $J'/J = 0.7$ and completely unambiguous at $J'/J = 1.0$, where the peak is at the expected triangular lattice value $(2\pi/3, 2\pi/3)$.

on the $3 \times 3$ lattice, and other limiting cases, for which analytic solutions are possible.

We imposed periodic boundary conditions and did simulations for different lattice sizes $L$ and different sets of the magnetic field $B_x$ and the coupling constant $J_{ij}$. For each simulation, we estimated the autocorrelation time $\tau$ and performed $5000\tau$ Monte Carlo sweeps for thermalisation and $10^5\tau$ to carry out the measurements. Results for the ferromagnetic case were on 30x30 lattices, and for the antiferromagnetic case on 27x27 lattices, unless otherwise stated.

### B. High Temperature Series Expansions

High temperature series expansions are based on a Taylor series expansion for the Boltzmann factor

$$\exp\left(-\beta\hat{H}\right) = \sum_n \frac{(-\beta)^n}{n\ !}\hat{H}^n \tag{6}$$

The trace of $\hat{H}^n\hat{O}$, where $\hat{O}$ is some local operator involves only a finite number of sites and hence can be evaluated, up to some order, by a straightforward though cumbersome method. A particularly efficient way of calculating high order series expansions for various extensive and intensive properties of the model in powers of $\beta$ is the Linked Cluster Method. The details of the technique can be found in the literature.[16,17] We have used this approach to obtain thermodynamic properties of the model for the triangular-lattice transverse-field Ising model with nearest neighbor and second neighbor interactions.

### C. High Field Expansions

Since the field term of the Hamiltonian is exactly soluble, one can also develop a series expansion in powers of $J/B_x$ for the ground state properties of the model. We have not done such a high order expansion at $T = 0$. However, we have used finite temperature, high field expansions to order $(J/B_x)^2$, to calculate entropy and other thermodynamic properties. These are useful in determining the isentropic contours at low temperatures and high fields. In general one expects very high order expansions to be valid down to any relevant phase transitions. Here, we expect a leading order expansion only to be valid down to $B_x \sim qJ$, where $q$ is the coordination number, or perhaps to somewhat smaller $B_x$ owing to the presence of frustration in the system.

## III. SQUARE TO TRIANGULAR LATTICE INTERPOLATION

In the introduction we briefly reviewed the physics of the square to triangular lattice interpolation of the classical antiferromagnetic Ising model. In this section, we generalize this problem to the case when a transverse

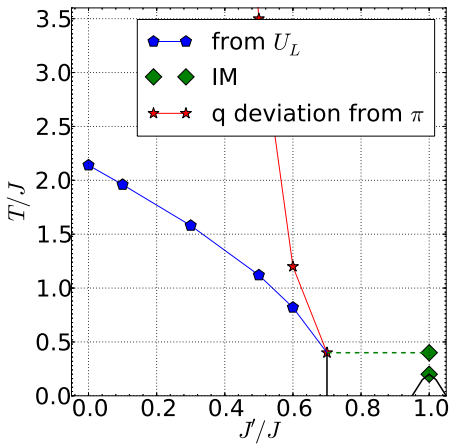


FIG. 3: (Color online) Phase diagram in the $T/J$ vs $J'/J$ plane. Pentagons are critical points representing a second order phase transition. Stars mark the disorder line at which the ordering wavevector shifts from $(\pi, \pi)$. It denotes the cross-over from the commensurate to the incommensurate region. Diamonds represent critical temperatures obtained by Isakov and Moessner in the triangular lattice limit. The dashed line separates a KT phase from a paramagnetic phase.

field $B_x$ is included, and connect to what is known about the problem with $B_x \neq 0$ in the triangular and square lattice limits. We consider a square lattice geometry with near-neighbor coupling $J$ and with an additional next-near-neighbor interaction $J'$ across one of the diagonals of each plaquette. In the limit $J' = J$ the triangular lattice is realized. As mentioned in the introduction, the nature of the phase diagram in the three dimensional space of $T/J, B_x/J, J'/J$ is already understood in certain limiting cases.

In the classical limit $B_x = 0$, Stephenson[21] solved the model analytically and calculated various correlation functions. Because the square lattic is bipartite, without loss of generality one may restrict consideration to a ferromagnetic choice $J < 0$. The critical temperature as a function of $J'/J$ is obtained from the transcendental equation[22]

$$t' = \frac{t^2 + 2t - 1}{t^2 - 2t - 1} \tag{7}$$

where $t' = \tanh(J'/T)$ and where $t = \tanh(J/T)$. This equation has solutions for which $T_c$ increases from the square lattice value $T_c/J = 2.269$ for additional ferromagnetic coupling $J' < 0$, and for which $T_c$ decreases for antiferromagnetic $J' > 0$. The critical temperature vanishes in the triangular limit $J' = -J$ and remains zero thereafter.

Similarly, in the $J'/J = 0$ plane, the square lattice has a second order phase transition with $T_c = 2.269$ at $B_x = 0$, and a $T_c$ which decreases as $B_x$ grows, ending in a Quantum Critical Point at $T = 0, B_x/J = 3.05$[16]. Finally, in the $J'/J = 1$ plane (antiferromagnetic Ising model in a triangular lattice in a transverse field) Isakov and Moessner argued[9] that turning on $B_x$ induced an order-from-disorder transition in which there are in fact two distinct (Kosterlitz-Thouless and clock) ordered phases. The maximal critical temperature is $T_c/J \approx 0.4$ at transverse field $B_x/J \approx 0.8$. Their study motivates us to pick a fixed value of $B_x/J = 1$ near this maximum to provide a detailed description of the evolution from square to triangular geometry.

Figure 1 shows an example of a Binder crossing which can be used to locate the transition temperatures when $J'/J$ is not too large. For the $J'/J = 0.5$ value shown, the crossing is well-defined and occurs at $T_c/J \approx 1.12$. For comparison, when the frustrating interaction and transverse field vanish ($J'/J = 0$ and $B_x = 0$) we have $T_c/J = 2.269$.

We can track $T_c$ from such Binder crossings only to $J'/J \approx 0.6$. The reason is that, as with the $B_x = 0$ case discussed by Stephenson, a disorder line where the structure factor peak shifts from $\mathbf{q} = (\pi, \pi)$ to incommensurate values approaches the phase transition line. The evolution of this incommensuration shift is seen in Fig. 2. A peak in $S(\mathbf{q})$ occurs at $\mathbf{q} = (\pi, \pi)$ up to $J'/J \approx 0.7$. At this point the peak moves away from the *Neel* value and evolves continuously towards the triangular-lattice $\mathbf{q} = (2\pi/3, 2\pi/3)$, as shown in Fig. 2.

Figure 3 shows the analog of Stephenson's classical Ising model disorder line, which demarks the switch from incommensurate peak in $S(\mathbf{q})$ to a commensurate AF peak, in the case of nonzero transverse field $B_x/J = 1$. It provides further insight into the failure of the Binder crossing procedure, which worked at $J'/J = 0.5$ as seen in Fig. 1. The phase above $T_c$ for $J'/J > 0.6$ no longer has a peak in $S(\mathbf{q})$ at $\mathbf{q} = (\pi, \pi)$, complicating the Binder scaling analysis. It is important to note that the disorder line is not a phase boundary, but rather a cross-over line that separates the commensurate from the incommensurate region. Below this line the short range order becomes pinned at $(\pi, \pi)$.

The interplay of this commensurate-incommensurate transition with Isakov-Moessner's observation of two phase transitions in the triangular-lattice limit ($J'/J = 1$) with the upper one being a Kosterlitz-Thouless transition remains a tricky one. Our suggested phase diagram is given in Fig. 3, where we show a dashed line connecting a multicritical point to the upper phase transition found by Isakov and Moessner. The lower transition may simply form a dome in the phase diagram near the triangular-lattice limit. As the magnitude of $B_x$ is reduced, the multicritical point will move closer to $J'/J = 1$ eventually ending at the highly degenerate point of the $T = 0$ triangular-lattice Ising model.

Figures 4 and 5 provide numerical evidence for the Kosterlitz-Thouless region in the interval $0.7 < J'/J < 1.0$ where the disorder line crosses the phase transition line. Figure 4 shows the spatial decay of the real space correlation function $C(\mathbf{r})$ for several temperatures at $J'/J = 0.8$. It is clear that at $T/J = 0.2$ and 0.4 that

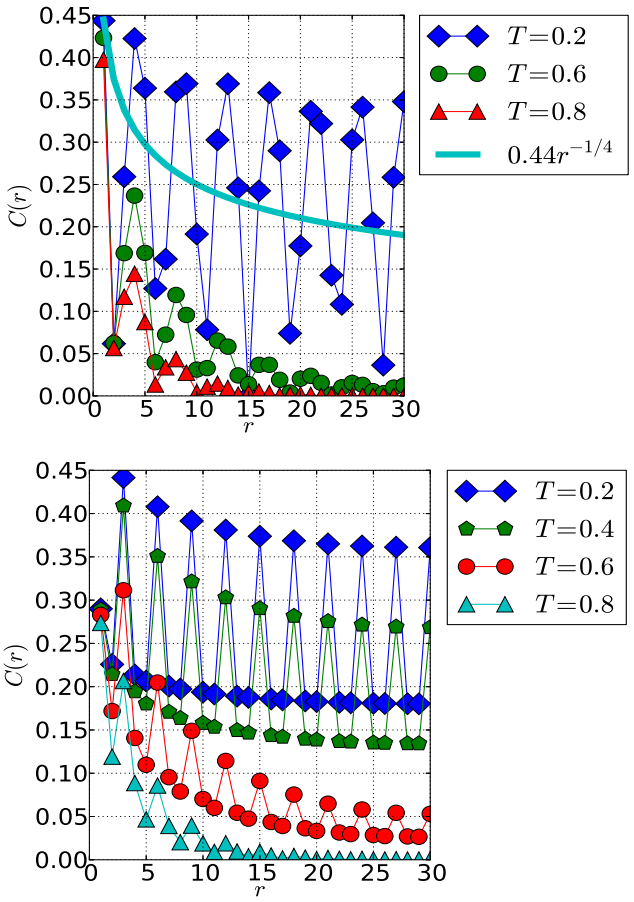


FIG. 4: (Color online) Correlation function $C(r)$ as a function of $r$ for several temperatures and transverse field $B_x/J = 1$. Upper Panel: $J'/J = 0.8$: The evolution of $C(\mathbf{r})$ with $r$ exhibits a clear qualitative difference for $T/J = 0.2$ and $T/J \geq 0.6$, and is consistent with power law decay in the lower temperature range, and an exponential decay at the higher temperatures. The function $C(r) = 0.44r^{-1/4}$ (solid line) shows the difference between power law nature of $C(r)$ at $T = 0.2$ and exponential decay for $T \geq 0.6$. The oscillations in $C(\mathbf{r})$ are associated with the fact the structure factor peak is not at $\mathbf{q} = (\pi, \pi)$. Lower Panel: $J'/J = 1.0$: Same as upper panel except in the triangular lattice limit. Oscillations are now at wavevector $\mathbf{q} = (2\pi/3, 2\pi/3)$.

$C(\mathbf{r})$ is decaying much more slowly than at $T'/J = 0.6$ and higher. While this change is suggestive of a phase transition to a long-range ordered phase, Fig. 5 puts things on a firmer footing. Here a log-log plot of the square of the structure factor versus linear lattice size gives the linear behavior which defines the Kosterlitz-Thouless phase for $T = 0.2$ and $T = 0.4$. The latter temperature has the power law slope $-1/4$ expected at $T_{\rm KT}$. At $T = 0.6$ the largest lattice sizes exhibit a decay with slope $-2$, a value generated by the normalization by $N = L^2$ in Eq. 3, since the spatial sum gives a contribution which is a lattice size independent constant at high temperatures owing to the exponential fall-off of

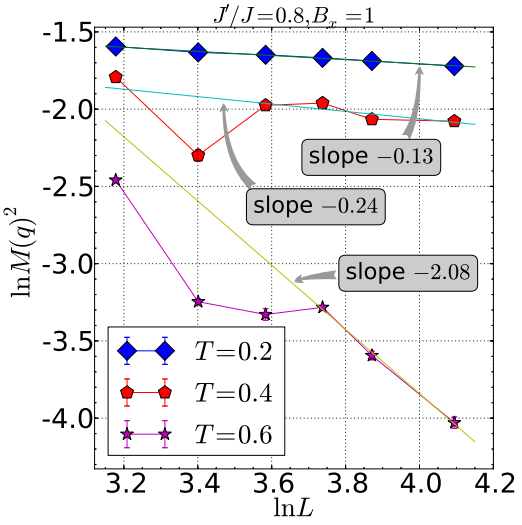


FIG. 5: (Color online) Below $T_{\rm KT}$ the structure factor decays as a power law with the lattice size, giving a straight line on a log-log plot, as shown occurs here for $T = 0.2$ and $T = 0.4$ at $J'/J = 0.8$ and $B_x = 1.0$. At higher $T = 0.6$ the slope simply reflects the lattice normalization in Eq. 3.

$C(\mathbf{r})$.

## IV. ISENTROPES ON THE NEAREST NEIGHBOR TRIANGULAR LATTICE

### A. Ferromagnetic Case

We begin by showing in Fig. 6(a) the entropy function for the ferromagnetic nearest-neighbor Ising model as a function of temperature and three values of transverse field. In this section, we will let $J$ denote the magnitude of the nearest-neighbor interaction. Fig. 6(b) shows the entropy function as a function of $B_x/J$ at four fixed temperature values. In both cases the symbols represent the results of the QMC simulations, while the solid lines give the high temperature series expansion results. The heat capacity as a function of temperature is shown in Fig. 7 for the same $B_x$ as the entropy plot. One can see a dramatic suppression in the specific heat peak as the quantum critical point $B_{xc} = 4/67$ is approached. In the thermodynamic limit, this must imply a sharp reduction in the amplitude for the specific heat divergence caused by the substantial loss of entropy before the transition to long-range order occurs.[28,29]

In Fig. 8 we show the phase diagram for the model together with the isentropic contours. While there is a very healthy amount of entropy in the system at the transition in small transverse fields (it is approximately 46 percent of the total entropy), when $B_x/J$ exceeds 4 the entropy at the transition is very small- less than 10 percent of the total entropy. The quantum critical point is known from previous studies to be at $B_x/J =$

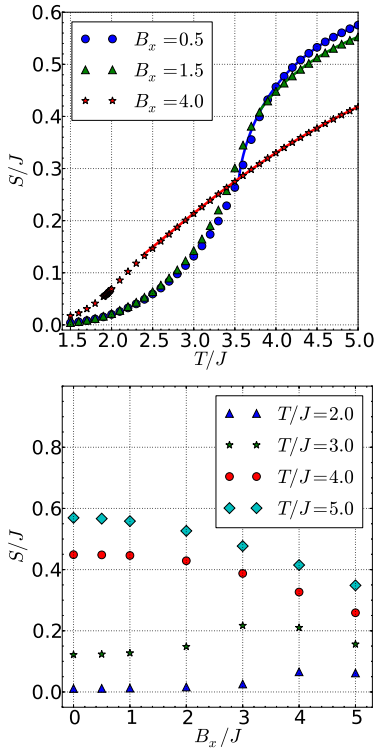


FIG. 6: (Color online) (a) Entropy $s$ versus temperature $T$ for several fixed values of the transverse field $B_x$. (b) Entropy $s$ versus transverse field $B_x$ for several fixed values of the temperature $T$. Squares (circles) are the results of CTQMC simulations on 27x27 lattice. Solid curves are series expansions.

4.67.[25,26] We found that, as the quantum critical point is approached and the transition temperature $T_c$ goes to zero, the entropy along the transition vanishes as $T_c^2$. This is consistent with general scaling arguments.[27] The appearance of minima in the isentropes near the phase transition line has been seen in a number of other classical and quantum models[30].

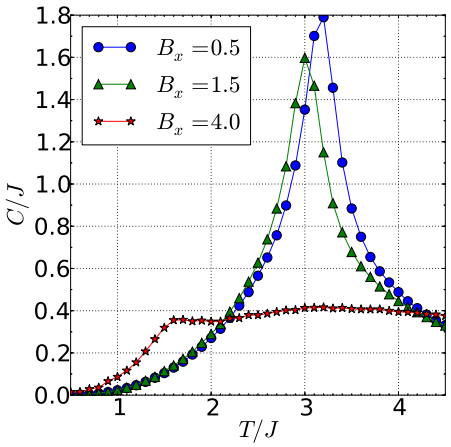


FIG. 7: (Color online) Specific heat $C(T)$ for the ferromagnetic nearest-neighbor model. The quantum fluctuations introduced by the transverse field $B_x$ reduce $T_c$ from the classical triangular lattice $T_c = 3.64$ until, for sufficiently large $B_x$, order no longer occurs at any finite $T$.

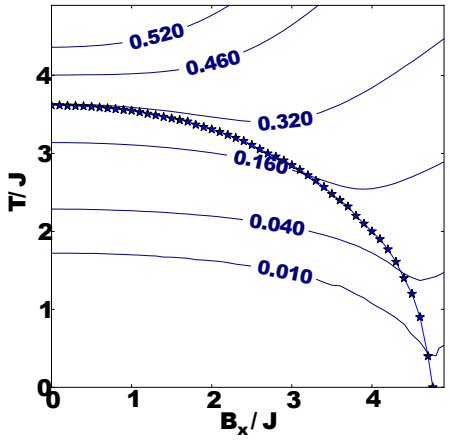


FIG. 8: (Color online) Phase diagrams and isentropes of the ferromagnetic triangular lattice model in the temperature $(T/J)$ vs megnetic field $(B_x/J)$ plane. Isentropes obtained from CTQMC on a 27x27 lattice and high temperature expansions. Phase boundary is obtained from the Binder cumulant.

### B. Antiferromagnetic nearest-neighbor triangular lattice model

We now turn to the antiferromagnetic nearest-neighbor Ising model on the triangular lattice in a transverse field. The entropy as a function of temperature at fixed $B_x$ and as a function of $B_x$ at fixed temperatures are shown in Fig. 9. The heat capacity for a few selected $B_x$ values as a function of temperatures is shown in Fig. 10. Note that, in this case, the peak in the heat capacity is associated with short-range order. Any long range order occurs only at much lower temperatures.

Fig. 11 shows the phase diagram and isentropes of the

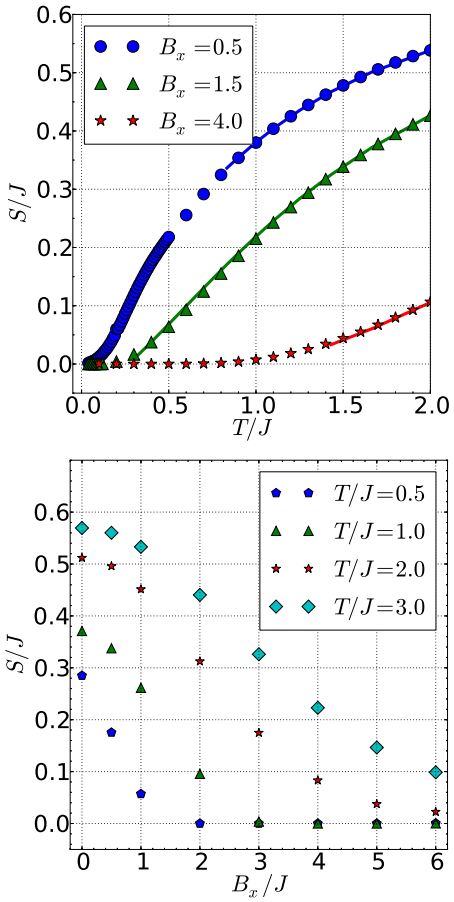


FIG. 9: (Color online) (a) Entropy $s$ versus temperature $T$ for several fixed values of the transverse field $B_x$. (b) Entropy $s$ versus transverse field $B_x$ for several fixed values of the temperature $T$. Squares (circles) are the results of CTQMC simulations on a 30x30 lattice. Solid curves are series expansions.

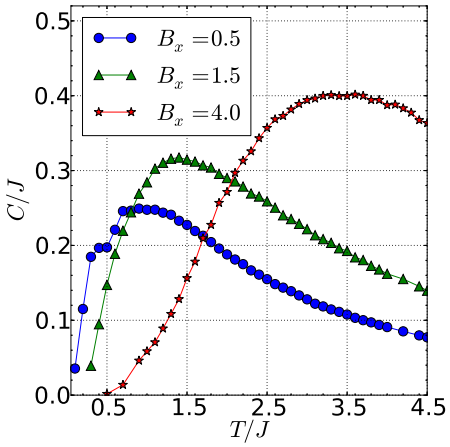


FIG. 10: (Color online) Specific heat $C(T)$ for the antiferromagnetic case. The peak in $C(T)$ is much broader than when $J < 0$, but shows a similar suppression towards $T = 0$ as $B_x$ grows.

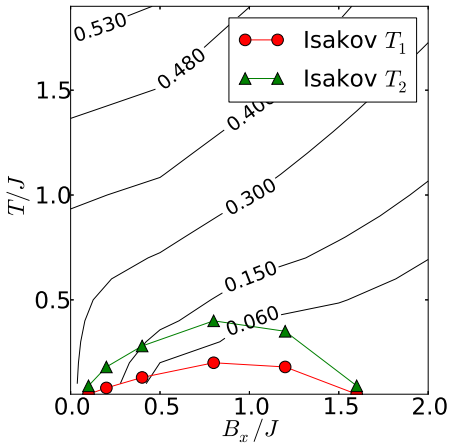


FIG. 11: (Color online) Phase diagram and isentropes of the near neighbor antiferromagnetic case obtained from CTQMC on the 30x30 lattice in the $T/J$ vs $B_x/J$ plane and high temperature expansions. Phase diagram was obtained by Isakov and Moessner.

antiferromagnetic model. Here, the phase boundaries showing two transitions as a function of temperature are taken from the work of Isakov and Moessner. Note that the triangular lattice Ising model has a substantial ground state entropy, but that must be removed at $T = 0$ with quantum fluctuations. This means that all contours of constant entropy between the values of 0.320 and zero must originate from the $T = 0$, $B_x = 0$ point. That singular limit is difficult to approach numerically.

We see that a magnetic field of $B_x/J$ slightly less than unity leads to the largest transition temperature. But, at the transition the entropy is rather small- only about one tenth of the total entropy in the system. This shows that these phase transitions involve a very small fraction of the states and may not be easy to get to.

### C. Effect of Longer Range Interactions

In the NIST experiments[13], spin-1/2 Be ions in a Penning trap interact with long range interactions which fall off with a tunable power law $J_{ij} \propto 1/r_{ij}^a$ with $0 < a < 3$. This range of functional forms allows quantum simulations going from infinite range ($a = 0$) to Coulomb ($a = 1$), to dipole ($a = 3$). Because the interactions are antiferromagnetic as well as long-range, the experiments correspond to 'large-scale' frustration, and, ultimately, it is hoped they will allow the realization of associated novel (eg. spin liquid) phases. In this section we will extend our numerical work on the thermodynamics of the nearest-neighbor antiferromagnetic transverse field Ising model on a triangular lattice to include several

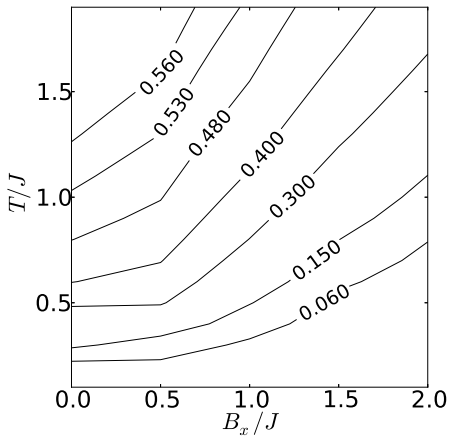


FIG. 12: Isentropes of the antiferromagnetic case with non-zero next near neighbor interaction $J' = J/\sqrt{3}$[1.4]. The change from Fig. 11 with $J' = 0$ is minimal. In particular, the key message is that the entropy values remain low in the region where phase transitions might occur.

realizations of longer ranged interactions. While we will not study systems with $J_{ij}$ non-zero between all pairs, these simulations give first indications of the evolutions of the entropy in situations with large-scale frustration.

The isentropes with a non-zero next-nearest neighbors interaction $J'$ are shown in Fig. 12. At low transverse fields this changes the isentropes as the tremendous ground state degeneracy of the nearest-neighbor Ising model is now lifted. However, at and above a transverse field of $B_x/J \approx 1$, the isentropes are very similar to the nearest-neighbor case and phase transitions would only occur at very low values of the entropy.

## V. CONCLUSIONS

In this paper we have provided quantitative results for the thermodynamics and phase transitions of the Ising model in a transverse field, with an emphasis on frustration and the effect of longer range interactions. For the isotropic triangular-lattice model, we have studied the entropy function for both ferromagnetic and antiferromagnetic exchange interactions. Using Quantum Monte Carlo simulations together with high temperature expansions and high field expansions, we have obtained the contours of constant entropy in the temperature, transverse-field plane. Our main conclusion is that phase transitions in the frustrated antiferromagnetic model occur at very low entropy compared to the unfrustrated case and these results are not substantially altered by adding weaker further neighbor exchange interactions.

We have presented a study of the quantum Ising model on the anisotropic triangular lattice that interpolates between the square and triangular lattice limits that yields new results for the phase diagram and thermodynamic properties. This model, with frustrating antiferromagnetic interactions, raises many subtle issues and presents a real challenge to any computational study. We first obtained the disorder line where the short-range order moves away from $(\pi, \pi)$. Unlike the $B_x = 0$ case studied by Stephenson, in presence of a transverse-field, the ground state order does not stay at $(\pi, \pi)$ all the way from the square-lattice ($J' = 0$) to the triangular-lattice ($J' = J$) limit. The disorder line crosses the phase transition line near $J'/J = 0.7$ and heads sharply towards $T = 0$. While it represents a crossover from short-range commensurate to short-range incommensurate order above this crossing, it presumably becomes a phase transition line separating long range commensurate order from power-law incommensurate order. At $T = 0$, it should turn into a Lifshitz point marking the onset of incommensurate long-range order.

Once the system has incommensurate order, the Binder ratios no longer show size independent crossings and it is difficult to determine the transition temperature for the expected Kosterlitz-Thouless phase. Rather than study many $J'/J$ values, we focused on $J'/J = 0.8$. We found that as the temperature was reduced there was a sharp change in the nature of spin-spin correlation functions between $T = 0.6J$ and $T = 0.2J$. The correlations are very small at large distances and consistent with exponential decay at $T = 0.6J$, whereas at $T = 0.2J$ they remain substantial at the largest distances accessible to our simulations and only a close inspection shows a power-law decay. A peak in the structure factor also moves with the size of the system making it difficult to precisely locate the transition temperature. At $T = 0.4J$, the correlation functions are consistent with a $r^{-1/4}$ decay, and hence we take this to be the transition temperature. At very low temperatures, the system may lock into other commensurate phases, as it does for the triangular-lattice case through higher order anisotropies, but those are beyond our simulation capabilities.

Cold atom experiments on the triangular lattice, transverse field Ising model are ongoing[13]. Our results provide quantitative data on the entropies required to reach possible phase transitions for different values of $B_x$. In addition to the connections of the present work to these experiments, and to triangular-square lattice interpolations of the Heisenberg model[19], similar experimental studies are now being undertaken on itinerant electron magnetism as realized in Hubbard models[31], as well as companion theoretical treatments[32]. The focus thus far has been on Dirac points on honeycomb lattices and topological features in the band structure. However, the behavior of spin correlations on such tunable lattices is one of the key goals of the next generation of experiments.

This work was supported by the University of California UCLAB program and by the NNSA under DE-NA0001842-0 and by the National Science Foundation

grant number DMR-1004231.


[1] T.D. Schultz and D.C. Mattis, Rev. Mod. Phys. **36**, 856 (1964).

[2] P. Pfeuty, Annals of Physics **57**, 79 (1970).

[3] M. Suzuki, Prog. Theor. Phys. **46**, 1337 (1971); and Prog. Theor. Phys. **56**, 2454 (1976).

[4] R.B. Stinchcombe, J. Phys. **C6**, 2459 (1973).

[5] H.W.J. Blöte and Youjin Deng, Phys. Rev. **E66**, 066110 (2002).

[6] S. Sachdev, *Quantum Phase Transitions*, Cambridge University Press, Cambridge, United Kingdom (1999).

[7] R. Moessner, S. L. Sondhi, and P. Chandra, Phys. Rev. Lett. 84, 4457 (2000).

[8] G.H. Wannier, Phys. Rev. **79**, 357 (1950).

[9] S.V. Isakov and R. Moessner, Phys. Rev. **B68**, 104409 (2003).

[10] P.G. de Gennes, Solid St. Comm. **1**, 132 (1963).

[11] Reference 4 contains an early list of systems related to the Ising model in a transverse field.

[12] E.E. Edwards, S. Korenblit, K. Kim, R. Islam, M.-S. Chang, J.K. Freericks, G.-D. Lin, L.-M. Duan, and C. Monroe, Phys. Rev. **B82**, 060412 (2010); K. Kim, S. Korenblit, R. Islam, E. E. Edwards, M.-S. Chang, C. Noh, H. Carmichael, G.-D.Lin, L.-M. Duan, C.-C. Joseph Wang, J.K. Freericks, and C. Monroe, New J. Physics **13**, 105003 (2011); and R. Islam, E. E. Edwards, K. Kim, S. Korenblit, C. Noh, H. Carmichael, G.-D.Lin, L.-M. Duan, C.-C. Joseph Wang, J. K. Freericks, and C. Monroe, Nature Communications **2**, 377 (2011).

[13] J.W. Britton, B.C. Sawyer, A.C. Keith, C.-C. Joseph Wang, J.K. Freericks, H. Uys, M.J. Biercuk and J.J. Bollinger Nature **484**, 489 (2012).

[14] S.M.A. Tabei, F. Vernay, and M.J.P. Gingras, Phys. Rev. **B77**, 014432 (2008); S.M.A. Tabei, M.J.P. Gingras, Y.-J. Kao, and T. Yavors'kii, Phys. Rev. **B78**, 184408 (2008).

[15] For a recent comprehensive review see A. Dutta, U. Divakaran, D. Sen, B. K. Chakrabarti, T. F. Rosenbaum, G. Aeppli, cond-mat:arXiv:1012.0653.

[16] J. Oitmaa, C. Hamer and W-H. Zheng, *Series Expansion Methods for strongly interacting lattice models*, (Cambridge University Press 2006).

[17] M.P. Gelfand, and R.R.P. Singh, *High-order convergent expansions for quantum many particle systems*, Advances in Physics, **49** N1:93-140 (2000).

[18] A. W. Sandvik, Phys. Rev. **E68**, 056701 (2003).

[19] See for example, Zheng Weihong, Ross H. McKenzie, and Rajiv R. P. Singh, Phys. Rev. **B59**, 14367 (1999).

[20] W. Selke and L. N. Shchur, Phys. Rev. **E80**, 042104 (2009).

[21] J. Stephenson, J. Math. Phys. **5**, 1009 (1964); *ibid.* **11**, 420 (1970); *ibid.* **11**, 413 (1970).

[22] T.P. Eggarter, Phys. Rev. **B12**, 1933 (1975).

[23] P. Bak, Rep. Prog. Phys. **45**, 587 (1982).

[24] W. Selke, Physics Reports **170**, 213 (1988).

[25] J. Oitmaa, C. J. Hamer and Z. Weihong, J. Phys. A: Math. Gen. **24**, 2863 (1991); H-X He, C. J. Hamer and J. Oitmaa, J. Phys. A: Math. Gen. **23**, 1775 (1990).

[26] H. Reiger and N. Kawashima, Eur. Phys. Jour. **B9**, 233 (1999).

[27] L. Zhu, M. Garst, A. Rosch and Q. Si, Phys. Rev. Lett. **91**, 066404 (2003).

[28] P. Sengupta, A. W. Sandvik and R. R. P. Singh, Phys. Rev. **B68**, 094423 (2003).

[29] J. Merino and R. H. McKenzie, Phys. Rev. Lett. **87**, 237002 (2001).

[30] J.D. Cone, A. Zujev and R.T. Scalettar, Phys. Rev. **B83**, 045108 (2011).

[31] L. Tarruell, D. Greif, T. Uehlinger, G. Jotzu, and T. Esslinger, Nature **483**, 10871 (2012).

[32] N. Bluemer, C-C. Chang, and R.T. Scalettar, unpublished.